



Effect of corrosion rates of preheated *Schinzochytrium* sp. microalgae biodiesel on metallic components of a diesel engine

Babalola Aisosa Oni ^{a,b,*}, Samuel Eshorame Sanni ^b, Benjamin O. Ezurike ^c, Emmanuel Emeka Okoro ^d

^a Department of Chemical Engineering, China University of Petroleum, Changping, Beijing, PR China

^b Department of Chemical Engineering, Covenant University, Km 10 Idiroko Road, Ota, Nigeria

^c Department of Mechanical/Mechatronics Engineering, Alex Ekueme Federal University Ndufu – Alike, Nigeria

^d Department of Petroleum Engineering, University of Port Harcourt, East-West Road, Choba, Nigeria

Received 6 July 2021; revised 26 November 2021; accepted 1 January 2022

Available online 13 January 2022

KEYWORDS

Biodiesel;
 Corrosion;
 Diesel engine;
 Fuel degradation;
 Microalgae biodiesel, Metals

Abstract Hitherto, the myriad of researches conducted on biofuels coupled with their poor oxidative stabilities, show that none of these studies has considered monitoring the corrosive effects of *Schinzochytrium* sp. microalgae biodiesel on diesel engines. In this study, corrosion behaviors of mild steel (MS), aluminum (Al) and copper (Cu) were compared via immersion tests in preheated *schinzochytrium* sp. microalgae biodiesel and its blends at room temperature and 60 °C for 1200 h. Property-variation of the individual/blended fuels, corrosion rates/products of the metals, and their morphologies were examined. For the metals, the corrosion rates are in the order of Al < MS < Cu at room temperature and 60 °C. The degraded properties and corrosion rates of the metals in the diesel fuel (B-100) and biodiesel fuel-blends, were seen to be minimal relative to those of neat biodiesel (D-100). The morphologies of the metals in contact with the fuels, showed substantial variation in surface properties for the Al, MS and Cu specimens. Furthermore, of all the three metals, copper was most prone to biodiesel corrosion. Hence, the results suggest the need to anticipate a future where the use of corrosion inhibitors for preventing engine-part degradation induced by bio-fuels becomes a reality.

© 2022 THE AUTHORS. Published by Elsevier BV on behalf of Faculty of Engineering, Alexandria University. This is an open access article under the CC BY-NC-ND license (<http://creativecommons.org/licenses/by-nc-nd/4.0/>).

Abbreviations: D -100, Biodiesel fuel; B - 100, Diesel fuel; Al, Aluminum; Cu, Copper; BD-50/50, Diesel/ biodiesel blend (50:50); TAN, Total acid number.

* Corresponding author at: Department of Chemical Engineering, China University of Petroleum, Changping, Beijing, PR China.

E-mail address: babalola.oni@covenantuniversity.edu.ng (B.A. Oni).

Peer review under responsibility of Faculty of Engineering, Alexandria University.

1. Introduction

Today's biodiesel physical and chemical properties are almost similar to those of petro-diesel hence, biodiesel is considered a good alternative to petrol-diesel. Biodiesel is a promising fuel for the future since it can be used with some form of modifica-

<https://doi.org/10.1016/j.aej.2022.01.005>

1110-0168 © 2022 THE AUTHORS. Published by Elsevier BV on behalf of Faculty of Engineering, Alexandria University. This is an open access article under the CC BY-NC-ND license (<http://creativecommons.org/licenses/by-nc-nd/4.0/>).

tion for any diesel engine [1]. In its pure form, biodiesel is somewhat chemically stable, however, during utilization, storage, and transportation, it degrades through microbial oxidation, moisture absorption, and other contaminants such as condensed water, which is a primary corrosion stimulant [2–3]. Apparently, biodiesels have displayed several advantages compared to those diesel fuels. Despite its major advantages, biodiesel has some shortcomings which include instability, corrosion, and other environmental issues [1,4], such as lower fuel economy (i.e., approximately 10% reduction on an energy basis) and slightly higher fuel density [5], poor atomization, lower fuel pours and cloud points, piston-ring sticking, higher NO_x emissions, potential corrosion to engines metal components, and higher problems of cold-starting [2,6]. Higher density, viscosity, and surface tension in biofuels result to evaporation and poor atomization in diesel engines.

Brake thermal efficiency (BTE) shows how effective a fuel is burnt in the chamber, which converts heat to work. Increase in BTE result to low brake specific fuel consumption (BSFC)[1,6]. The combustion duration and intensity are assessed from an engine's heat release rate, which is vital for combustion mechanism in diesel engines. For NO_x emissions to be reduced, it is important to reduce the ignition delay which is very important in engine combustion [2,5]. Generally, factors such as fuel type/quality, air – fuel ratio, fuel atomization, intake air pressure, engine speed and temperature affect the ignition delay [1,3,6].

The deposit formation of CI engines run with biodiesel, is an important factor which needs to be considered. Hoang and Pham [7] established the impact of preheated jatropha oil deposited on the piston crown operated after 300 h. Their result showed that the deposits from the oil were more than those of conventional diesel. Crude palm oil was used by Fazal et al. [8] in diesel engine operated at 500 h, they reported a deposit formation in the fuel injector and valve. Additionally, the scratches on the corrosion of piston rings, cylinder, jam valves, were also mentioned. Comprehensive works on the relationship between soot emission and carbon blacks' deposits, were also established by refs.[6,8,9].

Regarding the degradation of lube oil in compression ignition engines running on biofuels, there exist a relationship between deposit formation, lube oil degradation, and engine performance.

Singh et al [9] demonstrated that soot, deposits, that occur as a result of incomplete combustion in the chamber due to low heat supply which provide energy in a combination of the blow-by gases or the scrape of deposits and metallic components latching on the wall of the chamber through the piston motion were all moved into lube oil of diesel engines leading to oil contamination and degradation. Thus, a reduction of the working time of lube oil of diesel engines running on jatropha oil (400 h) compared to 512 h of working time of diesel engines fueled with diesel oil was reported by ref. [10]. In addition, the reduction of the anti-wear effectiveness of lube oil of diesel engines as a result of the intermingling of soot and deposits with the additives in lube oil leading to an increase in the abrasion of piston-cylinder was specified by refs. [8–10]. Apparently, the metallic components and material debris produced by the wear and abrasion process caused the damage of engines operated under the aforementioned conditions of lube oil breakdown [11]. According to Hoang [12], the presence of metal concentrations in lube oil changes the lube oil properties

such as density and viscosity, leading to problems related to the operations of the pump network. Therefore, the concentrations, viscosity, and density of the metallic particles is important in assessing the quality of lube oil after a certain period of operating the engine.

The percentage free fatty acids and water in biodiesel, makes it highly corrosive relative to diesel fuel, hence the need to regulate these undesirable components in the fuel [1]. Metallic corrosion induced by metal-contact with biodiesel, deteriorates the properties of the fuel, which in turn reduces the life span of metal parts, thereby affecting the performance of the engine [13]. The corrosion rate of engine parts depends on the biomass/feedstock from which the biodiesel is produced and its physicochemical properties [5].

Based on literature, all metals have the tendencies to become oxidized/dissolve when in contact with an electrolyte/solution. Though, the mass and the corrosion rates of metals differ owing to the difference in nature of the metal species/ions as well as their wear resistances [6,10,14,15]. These factors are also highly reliant on the oxidation potential the metals, abrasive tendencies, as well as fuel properties. Generally, when a metal is in contact with fuel, it may result in corrosion [5]. Due to this reason, manufacturers are faced with the challenge of combatting failure of the mechanical parts of diesel engines operating on biodiesel fuel [6]. These parts are the static components of the fuel system, for example, cylinder liner, filter, fuel line, injector, exhaust system, fuel intake, supply pumps, etc. Other metallic parts include valves, connecting rods, piston crowns, plungers, piston rings etc. [7]. Since biodiesel comprises of saturated and unsaturated fatty acids, over time, it is quite susceptible to oxidation [3,5]. Additionally, the corrosive ions that are contained in the water promote microbial growth and may hydrolyse the methyl esters with some modifications to its properties, such that it forms more corrosive fatty acids at the biodiesel-water interface. As a result of oxidation, insoluble gums, deposits and other secondary oxidation products, such as aldehydes, low molecular organic acids, and ketones which intensify the overall acidity and corrosiveness, are formed [8]. Besides, because of production imperfections, free water remains domicile in the biodiesel. These adversely affect the fuel properties and in turn corrode the vital fuel system/delivery-components such as injector pumps, fuel tubes and engine parts, thus causing longer ignition delays and less power and more smoke generation [9]. These undesirable outcomes which make biodiesel more hostile to automotive parts than conventional diesel–fuel are ascribed to the composition of the fatty acids as well as the hygroscopic characteristics and the presence of residual impurities in the fuel [4,7].

In this study, *Schinzochytrium* sp. microalgae biodiesel (SMB) was also considered due to its high fatty acid content as well as its potential for high biodiesel yield.

A good understanding of the corrosive properties of biodiesel is highly significant for ensuring the durability of engine-parts. Fazal et al., [13–14], compared the corrosion behaviour of Al, Cu and MS in both petroleum diesel and *Schinzochytrium* sp. microalgae biodiesel. Immersion tests in biodiesel and diesel were carried out at 80 °C for 1200 h. The corrosion rates were determined by weight loss measurements and changes on the metal surface. Optical microscopy and SEM-EDS were used to investigate the surface morphology of the engine-parts. The compositional characteristics such as acid concentration, oxidation level, water content, and the

incursion of metal species in fuels were studied using GCMS, ICP and TAN analyser, and FTIR, respectively. The degree of corrosion and change in fuel properties when exposed to metals is greater in biodiesel than in diesel fuels, according to findings from literature [8,11,15–16]. Stainless steel is highly resistant to biodiesel, whereas Cu and Al are more corrosion prone. Kaul et al. [17], investigated the corrosive properties of Mahua, Karanja, Jatropha curcas, and Salvadora biodiesels and compared them with those of diesel fuel. The result showed that the biodiesels (Jatropha curcas and Salvadora), were more corrosive for both ferrous and non-ferrous alloys compared to others. Due to oxidation and chemical reactions, the esters from the biodiesels were converted to mono-carboxylic acids such as formic, propionic acids etc. [18]. These acids increase the corrosion rates of the materials. In addition, the oxidation process is intensified by the water content of the biodiesel which results in high corrosion rates. Haseeb et al. [16] investigated the effects of palm biodiesel (B0, B50 and B100) on the corrosion level of leaded bronze and Cu under different conditions: (i) at room temperature, for 2600 h, and (ii) at 60 °C for 840 h. A TAN analyzer, MOA (multi-element oil analyzer) (TAN005 Paragon Scientific Ltd (Merck) UK. – ASTM -D664, were used to analyse the fuels in order to ascertain the acid concentration, corrosive impurities, oxidation potential and water content. The result shows that under the first condition, the corrosion rate of Cu in contact with B100 was 0.042mpy (milligram per year), and 0.018 mpy for bronze (B100). The rate of Cu corrosion for the second condition at B100 was 0.053mpy, while that of bronze corrosion for the B100 fuel was 0.023mpy.

Haseeb et al. [19], investigated the effects of different biodiesels at temperatures ranging from 15 to 40 °C on the corrosion behavior of the diesel engine piston fabricated with Al alloys using static immersion test (SIT). The results showed that corrosion occurred for the piston metal and piston liner as a result of its immersion in biodiesel (including Jatropha curcas L., (S1)-, Karanja (S2)-, Mahuan (S3)-, and Salvadora- Methyl esters (S4). For the piston liner, the corresponding weight losses are 3.6 mg for S1, 0.3 mg for S2, 0.3 mg for S3 and 6.1 mg for S4 which corresponds to 0.0117, 0.0058, 0.0058 and 0.0136 mpy when compared with diesel fuel which gave a corrosion rate of 0.0058 mpy. Piston metal gave high weight loss of 2.1 mg for S4 compared to 0.2 mg- S1 and 0.1 mg recorded for S2 and S3. The high TANs seen on S1 and S4 are indicative of their high corrosion rates. Fazal et al. [20] reported the corrosion properties of Cu, Al and stainless steel (SS) in Jatropha biodiesel. The rate at which the metals corrode was determined by weight loss and changes in the surface morphology by means of immersion test in biodiesel. Fuel samples were characterized before and after the immersion test, in order to ascertain the fuel's water content, viscosity and density. However, it was concluded that Cu had the highest rate of corrosion, with SS having low corrosion rate. The water content, density and viscosity, of the fuel samples increased after immersion, although, they were within the standard limits except water content.

The summary of corrosion rate (mpy) of some in biofuel produced from various oil as feedstock from previous works are shown in Table 1.

Some of the biofuels that have been used in CI engines include oil palm [3], soybean oil [4], corn bio-oil [1], sunflower oil [9], olive oil [17], castor oil [8], Jatropha curcas oil [13], pon-

gamia pinnata oil [5], linseed oil [21], milkweed seed oil [2], etc. Different parts of the engine are made from different materials (Table 2). Engine parts including piston rings, pistons, bearings, filters, fuel injectors, fuel liners, gaskets and fuel pumps come in contact with these fuels during operation [4]. Among these parts, copper-based alloys are the most affected by the fuel [15]. The use of biofuels has some favorable effects on the material of the engine [22].

Biofuels have better lubricity at room temperature and by increasing the concentration of biofuel, the deformation of worn surfaces decrease [14].

When producing biodiesel fuels, acid/alkali catalysts in the heterogeneous and homogeneous phase are used to enhance the esterification efficiency [27]. Sulphuric acid is one of such catalyst used. The acid in the biodiesel can corrode the engine parts. From literature, it can be deduced that microalgae biodiesel is a potential feedstock for diesel engines [17,28]. In general, it is worthy to note that additional investigations are vital on various aspects of biodiesel in general with regards to engine corrosion.

Furthermore, some researchers have discussed the use of several biodiesels as fuels in compression ignition engines, which may corrode the engine parts especially with the use of second-generation fuels for example (Jatropha etc.) but the corrosive properties associated with the use of *Schizochytrium* sp. microalgae biodiesel on CI engine-parts have not been investigated. *Schizochytrium* sp. microalgae has high oil content (i.e., about 78 percent of its dry weight), hence it is a potential material for biodiesel production [17,25,27,29]. Impurities such as fatty acids, unused catalysts, triglycerides, water, monoglycerides or diglycerides or triglycerides, etc. are usually associated with biofuels obtained from *Schizochytrium* sp. irrespective of the catalyst used in its production process. Of the impurities mentioned, unused catalysts are the most hostile in terms of increasing the corrosion tendencies of the materials of construction of CI engines [30]. Hence, the results of this research may be suggestive of the need to anticipate a future where the use of corrosion inhibitors as preventive measures for engine-part degradation induced by biofuels would be factored into their application in diesel engines. Also, in lieu of the several available researches that have been conducted on biofuels, only a little amount of literature was dedicated to monitoring the adverse effects imposed by poor oxidative stabilities of the fuels on diesel engines. Therefore, since *Schizochytrium* sp. microalgae biodiesel is a prospective biodiesel source that has not been given any consideration by previous studies, it then informed the need to explore its prospects as biofuel as well as under-study or monitor its corrosive effects on a diesel engine. Therefore, the aim of this research is to produce *Schizochytrium* sp. biodiesel and its blends as well as, monitor the corrosion rates of the preheated fuels in a compression ignition engine.

2. Mechanism of metal corrosion in biodiesel

In fabricating engine, ferrous and non-ferrous metals material are most commonly used [11]. The fuel delivery systems of the CI engine with common materials used in fabrication of the fuel system parts is illustrated in Fig. 1.

Metals such as Fe, Al and Cu as well as their respective alloys are somewhat susceptible to corrosion in biodiesel fuels.

Table 1 Weight loss and corrosion of alloys and metals in biofuels obtained at various feedstocks.

Type of biodiesel	Conditions of experiment		Corrosion rate			Reference
	Temp. °C	Time duration	Aluminum	Cu/Cu -alloy	Steel/steel-alloy	
Jatropha oil methyl esters	80	600.0	0.35 mmpy	0.920 mpy		[21]
	80	1600.0	0.000762 mmpy	0.0110 mmpy	0.0000406 mmpy	[17]
Sunflower oil methyl esters	Room temperature	3000	0.162 mpy	0.324 mpy	0.1701 mpy	[22]
	60	–	0.316 mpy	0.641 mpy	0.337 mpy	
Palm oil methyl esters	Room temperature	960		0.40 mpy	–	[16]
	60	2640.0	–	0.05 mpy (Cu)	–	[16]
	Room temp.	2640.0		0.02 mpy leaded bronze		[12]
	Room temp.	2880	0.17 mpy	0.04 mpy (Cu)		[23]
	Room temp.	2880		0.0180 (leaded bronze)		[23]
	Room temp.	2880		0.33 mpy (Cu), 0.21 mpy (brass)	–	[24]
	Room temp.	1440	0.1230 mpy		0.06 mpy	[8]
	Room temp.	600	–	6.80	–	[12]
	Room temp.	1200	–	9.70	–	[5]
	Room temp.	1440	–	23 µmpy	1.8 µmpy	[24]
	Room temp.	480	–	0.4507 mpy	0.0525 mpy	[17]
	Room temp.	960	–	0.9426 mpy	0.0688 mpy	[17]
	Room temp.	1400	–	0.9106 mpy	0.0695 mpy	[9]
	100	540	0.000929 mpy	0.000929 mpy	0.000188 mpy; 0.000625 mpy (galvanized steel)	[25]
Rapeseed oil methyl esters	43	1440	0.032 mpy	0.0233 mpy	0.01819 mpy (Mild steel) 0.00087 (Stainless steel)	[26]

Table 2 Characteristics of the diesel engine's materials of construction.

Engine parts	Materials
Fuel tank	Plastics and/or Steel
Fuel filter	Resin impregnated paper, paper, aluminium, plastic.
Gaskets	Copper, elastomer, paper, cork.
Fuel injector/ Valves	Stainless steel/Special alloy steels
Fuel feed pump	Copper-based alloy, Aluminium alloy, iron-based alloy
Fuel pump	Copper – based alloy, iron-based alloy, Aluminium alloy
Fuel lines and hoses	Rubber, steel, plastic
Nozzles/ bearings	Leaded bronze, Steel/White metal,
Pistons/Piston liners	Aluminium alloy/cast iron, Nickel alloy steel, cast iron, steel.

According to Ahmmad et al., [21], the corrosion phenomenon of the mechanical parts of a CI engine are classified into three,

namely, cosmetic, perforation and edge corrosion. The perforation mechanism is the most predominant of all the three categories. Additionally, galvanic corrosion was also reported by Squizzato, et al. [25]. In this corrosion phenomenon, biodiesel was found to be more corrosive than diesel fuel, due to the presence of, and electronegativity of O₂ in biodiesel. Consequently, the electrolytic dissociation of esters, water or acid in the biodiesel, into radical groups containing oxygen is the main factor that enhances the corrosiveness of biodiesel. Furthermore, the accumulation of anaerobic and aerobic microorganisms in biodiesel, can be considered the reason for the increase in biodiesel-acidity which in turn influence its corrosive ability [12,23,25]. Currently, much has not been done on unravelling the mechanisms responsible for the corrosiveness of metals in biodiesel. Fazal, et al. [20] demonstrated the corrosion mechanism of pitting corrosion of copper exposed to biodiesel at 80 °C. Pitting corrosion is regarded as more destructive compared to other forms of corrosion. Oxygen in biodiesel contacted with Cu-metal, can be converted to Cu₂O which is very unstable and may subsequently be converted to CuO [2,29]. CuO is the oxidized form of Cu-metal after long exposure to biodiesel and the steady disappearance of the Cu₂O layer (located between CuO and metallic copper), results in the formation of CuCO₃ [19]. The presence of CO₂, dissolved oxygen, RCOO – and moisture in biodiesel, may further intensify the corrosion rate of Cu in biodiesel, which

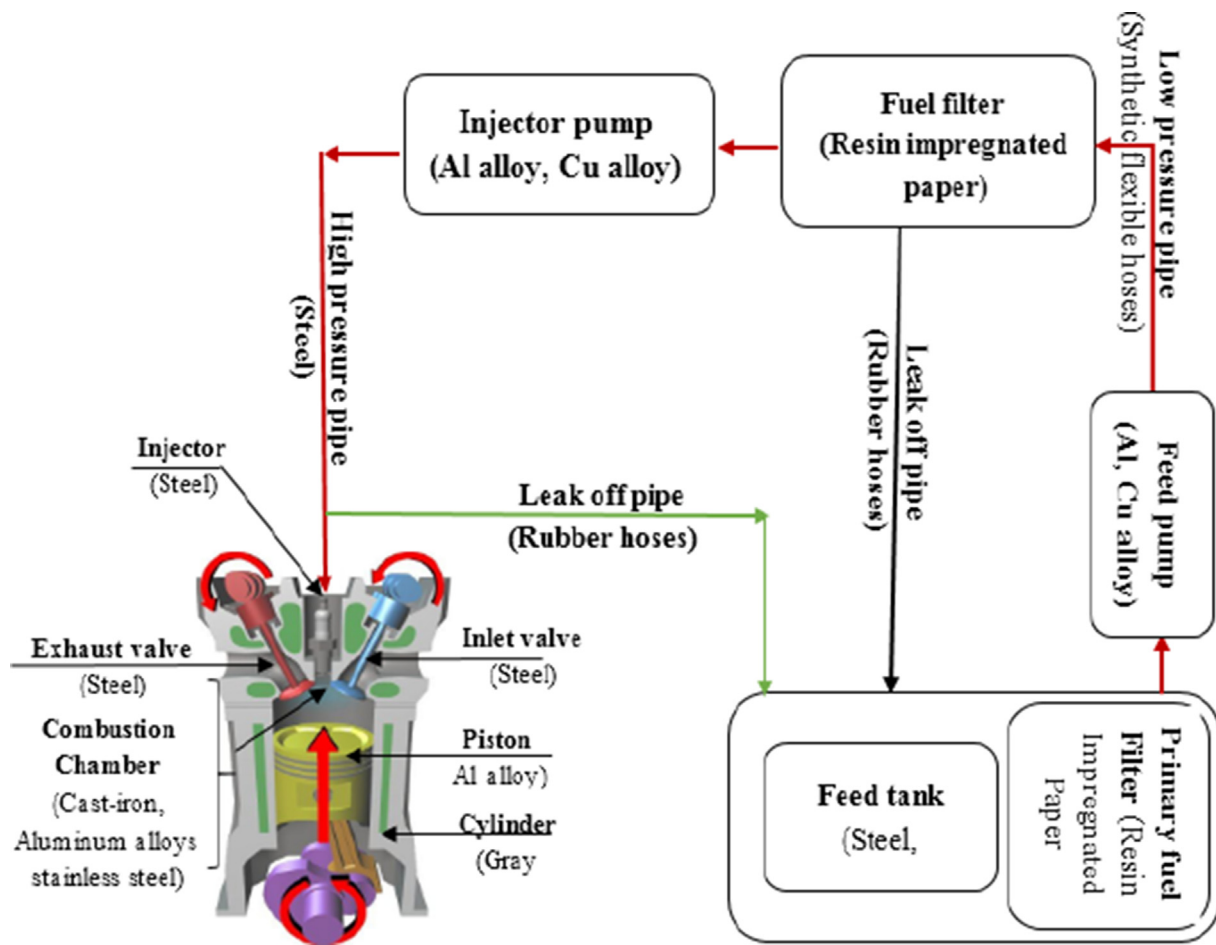
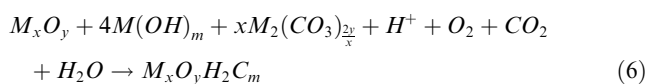
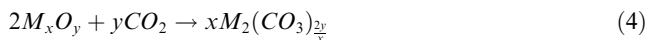
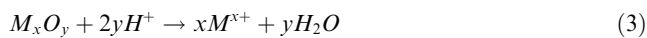
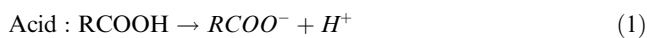


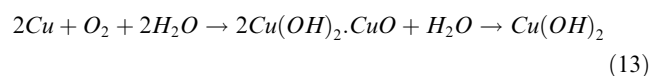
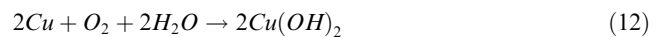
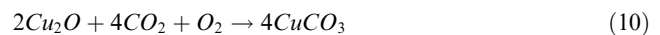
Fig. 1 A Typical fuel system of a compression ignition (Diesel) engine and common materials [6].

may also lead to the formation of carbonate and hydroxyl-based copper compounds ($\text{Cu}(\text{OH})_2$, CuCO_3 , $\text{Cu}(\text{OH})_2$, CuCO_3 ,) [16–20]. The mechanism of metallic corrosion is as illustrated in the reactions indicated in Eqs. (1)–(6) and the complex $\text{M}_x\text{O}_y\text{H}_z\text{C}_m$, M^{x+} , $\text{M}_2(\text{CO}_3)_{2y/x}$, $\text{M}(\text{OH})_m$ is the precursor for the product of corrosion [21–23].

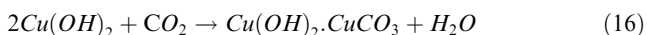
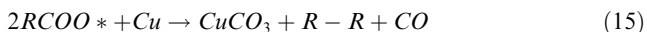
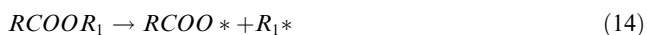


According to Gil et al. [24], the presence of a thin aqueous layer was responsible for the forming of the hydroxyl bonds for copper oxide. Fazal et al. [26] showed the relationship between different compounds produced as a result of Cu-exposure to biodiesel and the time of static immersion test. Based on the results, at the first 200 h of immersion testing, minute quantities of CuCO_3 , Cu_2O , $\text{Cu}(\text{OH})_2$ and CuO were

formed. When the exposure time extended to 300 h, the quantity/growth rate of CuCO_3 increased. Taking it further to 2880 h of Cu-exposure to biodiesel, the quantity of CuCO_3 formed was higher, thus shielding/suppressing the peaks associated with metallic Cu while minute quantities of other corrosion products were still traceable. In addition, reports have it that other Cu-based compounds maybe produced by additional oxidation of the above-mentioned oxides (Eqs. (7)–(13)).

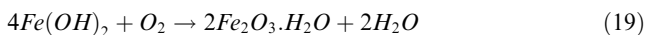
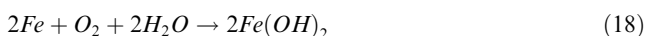
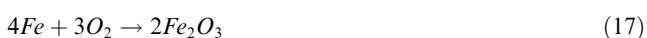


The generation of the RCOO^* radicals is responsible for CuCO_3 formation through the decomposition of ester (Eqs. (14)–(16))



The main component of steel is Iron (Fe) which is susceptible to corrosion, especially when exposed to biodiesel. Some of the corrosion products formed from iron include $Fe(OH)_3$, Fe_2O_3 , $Fe_2O_2CO_3$ which are traceable to the presence of water and oxygen in biodiesel [11,16]. The production of $Fe_2O_2CO_3$ is based on the reaction between $FeO(OH)$, and H_2CO_3 , however, $FeO(OH)$ is usually produced via the redox reaction occurring between either of any two of water, Fe, and O_2 . The adsorption of O_2 , water and CO_2 from air into biofuels may result in producing corrosive compounds, such as hydrogen carbonate, on the surface of steel [8].

The corrosion mechanisms for iron-based alloy in contact with oxygen and biodiesel are as shown in Eqs. (17)–(21).



Residues of alkaline such as NaOH and KOH, employed as catalysts for producing biodiesel fuels at the transesterification stage are usually the causes corrosion in aluminium and aluminium-based alloys [15,18]. Based on some studies, the effect of biodiesel-influenced corrosion on aluminium is relatively insignificant compared to its effect on copper and steel.

3. Materials and method.

3.1. Preparation of *Schinzochytrium* sp. microalgae biodiesel.

The microalgal strain used for this study is the *Schinzochytrium* sp. microalgae harvested from a swampy area/forest about 15 km from Covenant University, Ota, Nigeria. The samples were sun-dried for 3 days (72 h) so as to remove the water present. The dried samples were pulverised with mortar, grind to powder and sieved with a sieve mesh of 120 μ m. The ground algae were then placed in an oven for 1 h and maintained at 70 °C to further remove moisture. 1000 g algae-powder was stored in a sealed container and placed in a desiccator. The dried algae were then mixed with 500 mL hexane in a 2000 mL separating funnel for oil extraction and the resulting mix was allowed to settle for 48 h in order to allow for separation into two distinct layers. The organic phase containing the oil was emptied in a 1000 mL beaker. Separation was carried out between the algal oil and the residual constituents by filtration; the oil recovered was then weighed. Thereafter, the oil extracted was heated at 69 °C in a water bath in order to vaporize hexane (Fig. 2a). Fig. 2b shows the *Schinzochytrium* sp. biodiesel methyl esters with glycerine

Sodium methoxide catalyst was used for the production of the biodiesel. The catalyst prepared was slowly added to the filtered oil and heated at 55 °C, while stirring for about 30 min;

mixing continued for about 20 h in order to ensure homogeneous mixing and for efficient separation of the glycerol and biodiesel. The glycerin was collected at the base of the funnel while the Crude *Schinzochytrium* sp. biodiesel was collected at the top of the funnel. A pure Crude *Schinzochytrium* sp. biodiesel was obtained and kept for use. The Biodiesel was kept in an inert atmosphere prior to and after use, for water absorption and oxidation and prevention.

3.2. Static immersion test on fuel

Three fuels, B100 (100% diesel), B50-D50 (50% biodiesel, 50% diesel) and D100 (100% biodiesel), were then prepared for use in the static immersion test (SIT). In order to prevent reactions between the blends and atmospheric oxygen, the biodiesel-blends were kept for 25 min prior to the commencement of the experiment and stored in sealed glass bottles.

Some of the impurities present in the biodiesel include, triglyceride (~0.03%), free glycerol (~0.014%), diglyceride (~0.11%), water (~277 ppm), monoglyceride (~0.77%) and glycerol (~0.20%). Approximately 0.57 mg KOH/g was recorded as the acid value of the algal bio-oil which falls within the EN 14214 standard limit.

3.3. Preparation of metal samples

Some metallic parts of the Petter PH1W diesel engine, were cut into pieces of size 13 mm \times 8 mm \times 3 mm (area 0.0369 dm²) by milling and machining. After machining and polishing, the metal-pieces, were degreased with isopropanol-xylene mixture of ratio 1:1. The samples were weighed up to an accurate value of 0.1 mg before being exposed to the various biodiesel and diesel fuels. Corrosion characteristics of Cu (99.99%), Al (99% pure commercial grade) and 315 mild steel containing 19% Cr, 10% Ni, 2% Mn, 3% Si and 0.09% C in contact with diesel fuel and *Schinzochytrium* sp. biodiesel were examined by static immersion test at room temperature and 60 °C for 1200 h.

During the test process, fuels were constantly stirred at 200 rpm. The test coupons of Cu (17.4 mm diameter \times 2 mm thickness), Al (22.5 mm diameter \times 2 mm thickness) and Mild steel (15 mm diameter \times 2 mm thickness) were round bar pieces obtained by machining and grinding. A hole of 2 mm diameter size was used to suspend the specimens in the biofuels which was drilled at the edge. Before carrying out the immersion tests, the treated coupons were polished with SiC abrasive papers, washed and was lastly degreased with acetone. After which, they were dipped in 10% sulfuric acid at room temperature for 5 min and finally washed in deionized water. In the same way, after exposure, in order to remove the corrosion products, a polymer brush was used to lightly clean-up the surfaces of samples in a stream of water to avoid abrading the original surface. Before and after exposing the test coupons into different test fuels, their weights were determined with a weighing balance (METTLER AT 400 electronic analytical balance, IET, US) Duplicate coupons were immersed in each of the test-fuels. For each coupon, the loss in weight of the metals were recorded. Finally, corrosion behavior was examined by measuring the corrosion rates and changes in surface morphology. The weight loss measurements

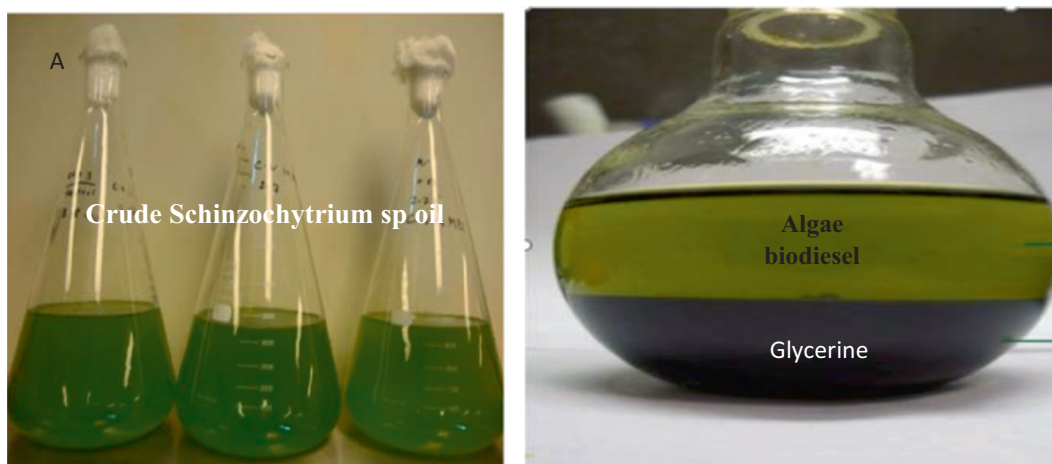


Fig. 2 (a) Crude *Schinzochytrium* sp.-oil (b) *Schinzochytrium* sp. biodiesel methyl esters with glycerine.

obtained for the duplicate test-coupons were used to calculate the corrosion rate (mpy) as given by Eq (22).

$$\text{Corrosion rate (CR) (mpy)} = \frac{W534}{DAT} \quad (22)$$

where CR = corrosion rate in millimeter or inch per year, W = weight loss (mg), D = density (kg/m^3), A = exposed surface area (sq. in.) and T = time of exposure (h). Characterization of the metals was done in order to examine the surface morphologies of the metals by optical microscope (OM), Atomic force Microscopy (AFM) which consists of a 3100 dimension with Nanoscope III controllers fitted with a silicon nitride DNP-S tip. Other analyses include Transmission electron microscopy (TEM), selected area electron diffraction (SAED), X-ray diffraction (XRD) and scanning electron microscopy (SEM)/EDS) model FEI-QUANTA 2000. The biofuels were analyzed with an Agilent 7000 D Triple Quadrupole GC/MS, Agilent triple-axis HED-EM with extended-life EM and dynamically ramped iris, with dimensions of $35 \text{ cm} \times 86 \text{ cm} \times 47 \text{ cm}$. It has an IDL sensitivity of 2 fg OFN injected: IDL $\leq 4 \text{ fg}$; oven temperature $30 \text{ }^\circ\text{C}$, with thermo conductivity detector (TCD) limit of 60 mA which helped to investigate the compositional change in the biodiesel. The biofuel's contaminated properties were measured by determining the total acid number (TAN), moisture content, density, oxidation stability and viscosity of the biofuels. The image of the test engine is illustrated in Fig. 3.

4. Uncertainty analysis of engine experimental results

Physical parameters and the operating of compression ignition engines can result to some uncertainty during the experimental results. Thus, uncertainty analysis is vital in an experiment for the purpose of accuracy. The technique for evaluating uncertainty analysis, as shown in Eq. (23).

$$y_R = \left(\left(\frac{\partial R}{\partial X_1} y_1 \right)^2 + \left(\frac{\partial R}{\partial X_2} y_2 \right)^2 + \dots + \left(\frac{\partial R}{\partial X_n} y_n \right)^2 \right)^{\frac{1}{2}} \quad (23)$$

where, y_R is the total uncertainty, the uncertainties of the independent engine operating parameters are y_1, y_2, \dots, y_n and

R is computed for the independent engine operating parameters at X_1, X_2, \dots, X_n .

5. Results and discussion

The properties of the *Schinzochytrium* sp. microalgae biodiesel (SMB) are as shown in Table 3.

All the parameters determined in Table 3 were in accordance to the ASTM standard procedures.

5.1. Corrosion rate

Fig. 4, shows the corrosion rates of the exposed metals to the different fuels i.e., the corrosion rates of the metals in the conventional diesel (B100), biodiesel (D100) and diesel/biodiesel blend (B/D 50/50) respectively. Fig. 4 (A-D) are illustrations of the rates of contamination of degradation, rate of corrosion of Al, Cu and MS at room temperature, the corrosion rates of Al, Cu and MS at $60 \text{ }^\circ\text{C}$ and the rates of degradation/contamination of the fuels at different times, respectively. The rate of contamination of biodiesel and its blend are more than that of the conventional diesel fuel at room temperature (Fig. 5A), this then informs that the purer the biodiesel, the more prone it is to contamination. At increased temperatures (Fig. 5A), all fuels, demonstrated increased degradation rates, which is also in line with the findings in ref. [13]. For the three metals, at room temperature, the rates of corrosion are in the following order of increased corrosion rates $\text{Al} < \text{MS} < \text{Cu}$ at $60 \text{ }^\circ\text{C}$ (Fig. 5 B). Also, at different temperatures, the rate of degradation of the diesel fuel (B100) is lower than those of the biodiesel (D100) and its blend (B/D-50/50). Considering Fig. 5C, the degree of corrosion of metals in the fuels is in the order of $\text{Al} < \text{MS} < \text{Cu}$ at both conditions i.e., at room temperature and $60 \text{ }^\circ\text{C}$, as illustrated in Fig. 5B and 4C respectively, this corroborates the findings of several authors [10,11,16,17,18,20]; this is because, the corrosion products formed on the metals are more stable/protective at lower temperatures than at higher temperatures. The corrosion rates of Mild steel (MS) at room temperature are 0.11, 0.13 and 0.18 mpy for the B100, B/D -50/50 and D100 fuels, respectively.



Fig. 3 Image of the test engine.

Table 3 Fuel properties of *Schinzochytrium* sp. microalgae biodiesel.

Parameter	ASTM standards	SMB Diesel fuels
Density (kg/m ³)	D0445	881 819
Flash point (°C)	D93- 2A	160.4 63.1
Kinematic viscosity @ 40 mm ² /s	D445	2.56 2.70
Pour point (°C)	D97-05A	-2 -2
Cetane number	D613-84	56 54
Acid value mg KOH/gm	D664	0.57 -
Carbon residue (% mass)	D189, D4530	0.046 0.017
Water and sediment (% vol.)		0.050 0.008

Cursaru et al., [23], stated that biodiesels are more prone to contamination when exposed to metals, as a result of the presence of oxygen and water in biodiesel fuels, hence, in Fig. 5B, it can be seen that the recorded corrosion rates induced by the blended and pure biodiesels are higher than that of the diesel, which also compares favorably with the results of previous studies [5,11,17]. Furthermore, the degree of passivation is lower for MS relative to Al, however, despite its low passivation, MS is more corrosion resistant relative Cu (due to the lower passivation of Cu relative to MS), thus, the Cu metal corroded faster than Al and MS. The results of the corrosion

rate of MS in contact with the three fuels, as obtained at 60 °C are 0.2, 0.23 and 0.39 m/y for the B100, B/D 50/50 and the D 100 fuels respectively; however, these values are less than those recorded in the findings of refs. [15,16], hence, an indication that the biofuel and its blend are more corrosive relative to the conventional diesel fuel when in contact with MS used.

Higher corrosion rates were recorded for the metals at increased temperatures, despite being warm at 80 °C, water molecules remain in liquid state, which may have imposed more thermal degradation/reaction between the metallic constituents and the fuels, compared to the effects recorded at 60 °C and lower temperatures (Fig. 5A). Generally, Mild steel (MS) contains 0.19 % C, 0.49 % Mn, 0.47 % Si and 98.8 % Fe, although the MS used in this research is about 0.21% C, 0.41% Mn and 99.4% Fe, which may have resulted in its improved resistance to corrosion relative to Cu at room temperature (Fig. 5 B) when compared to the results of previous studies [15,16].

In Fig. 5A, the highest corrosion rates (0.31, 0.37 and 0.69) were recorded for Cu when in contact with B100, B/D-50/50 and D100 respectively, as compared with Al and MS. At room temperature, the corrosion rate of copper in B/D -50/50 and D100 are 0.23 and 0.37 mpy, which are higher than that of the pure diesel B100 (0.15 mpy) (Fig. 5 B). However, the corrosion rates recorded in this study for Cu in contact with the B100 and B/D -50/50 fuels used in this study are lower than those recorded in previous studies [12,15,19,20]. Nevertheless, Haseeb et al. [10] obtained 0.0420 mpy for corrosion tests con-



Fig. 4 (a) Corrosion monitoring instrument. (b) Total acid number (TAN) tester.

ducted copper in contact with biodiesel at 25–30 °C for 2600 h. The observed low corrosion rate is as a result of the long immersion time (2600 h) and low temperature, which could have resulted in the formation of an oxide film that acted as an impervious layer for persistent metallic corrosion. Also, a maximum corrosion rate was observed for Cu at 600–1200 h, after which, the corrosion rate drops [14]. The corrosion rate of Cu obtained in this study at 60 °C for D100 (biodiesel) is lower than those of the biofuel and its blend as obtained in other related studies [13–17,21] (Fig. 5 C). At room temperature, the corrosion rate of Al was 0.14, 0.17 and 0.31 mpy when in contact with the B100, B/D –50/50 and D100 fuels, respectively. As reported by previous works [13,16,19], these values are lower, hence giving credence to the better properties of the biodiesel/biodiesel blended fuels used relative to those adopted in those studies. The corrosion rates of Al in B100 and B/D –50/50 at 60 °C compare favorably with those presented by Hu et al. [22] for biodiesel in contact with aluminum; however, these results are less than those reported by [26]. Based on the findings of Hu et al. [22], Al has a very great tendency to generate a metal oxide film/protective layer when in contact with oxygen from biofuel, which helps to impede high penetration of oxygen/interaction with the biofuel and thus lowers the corrosive influence of the fuel. At different times, i.e., 240, 480, 720, 960 and 1200 h, the corrosion rate increased with time, this is in agreement with the results in refs. [18,21]. At 1200 h, Fazal et al. [13,14] obtained 0.06 mpy degradation rate for biodiesel obtained from palm oil at 60 °C, whereas, based on this study, the degradation rate of all the fuels increased with time with the highest degradation rate recorded for the D100 fuel which is more prone to metallic interaction. The rate of degradation/contamination of diesel, the blended biodiesel and the pure biodiesel are as illustrated in Fig. 5D, where one can assert that the unblended biodiesel raises the oxidative potential or increases the tendency for contamination/degradation of the biofuel used; the results show higher degradation rates for pure biodiesel (B100) relative to that of B/D-50/50, owing to the influence of diesel fuel mixed with it

which helps to reduce the oxidative potential of the pure biofuel. However, due to the fact that blending of biofuels with conventional diesel fuels, offers some advantages, it then suggests that, an optimum concentration must be sought for optimal engine performance without jeopardizing the engine-life or durability of the engine parts.

5.2. Variation in fuel compositions and properties.

These properties include density, water content, total acid number (TAN), oxidation stability, viscosity.

5.2.1. The total acid number (TAN)

The degree of acidity/H⁺ concentration in a non-aqueous solution is termed TAN. The TANs of all the fuels at room temperature, before and after exposure to metal are as illustrated in Fig. 6. For the neat fuels, the recorded TANs are in the following order of increased TANs i.e., B100 (0.15 mg KOH/g acid) < B/D-50/50 (0.27 mg KOH/g acid), D100 (0.35 mg KOH/g acid), which then suggests that the neat/pure biodiesel is the most acidic of all the three fuels, while the B/D-50/50 fuel is more acidic with respect to B100, hence the reason for the recorded high corrosion rates of the metals in contact with the fuels as shown in the fuel-metal system vs rate of TAN-plot in Fig. 6. At room temperature, the TAN of each metal (Al, Cu and MS) in contact with B100, B/D-50/50 and D100, shows that the TANs are in the following increasing order of magnitude for the fuel-metal systems: Al (0.16, 0.80 and 1 mg KOH/g acid) < MS (0.15, 1 and 1.2 mg KOH/g acid) < Cu (0.15, 1.42 and 1.5 mg KOH/g acid), for the Al-B100/B/D-50/50 and D100 systems, MS- B100/B/D-50/50 and D100 as well as the Cu- B100/B/D-50/50 and D100, respectively. The results also confirm how stable the neat diesel-fuel is to oxidation/contamination/degradation as its TAN value = 0.15 mg KOH/g acid. According to the ASTM D6751 standards, the permissible TAN limit of diesel fuel is 0.8 mg KOH/g, which then suggests that the TAN of the D100 and

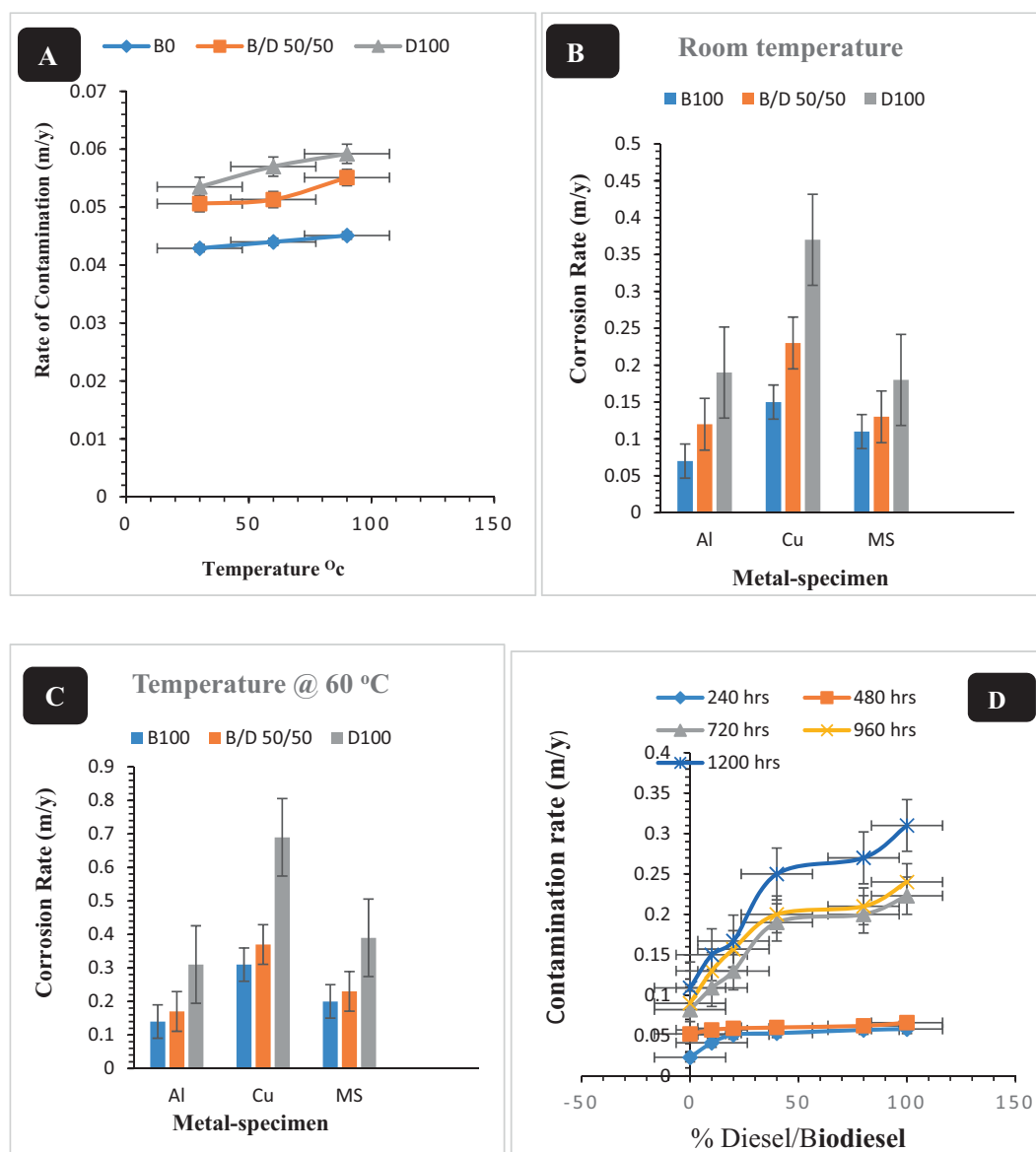


Fig. 5 Corrosion profile (A) at 40, 60 and 80 °C (B) at room temperature (C) at 60 °C (d) at different time.

B/D-50/50 blend exceeded the ASTM standard TAN-limit after having contact with the metal surfaces at room temperature. Another reason for the increased TAN rates of the D100- and BD-50/50- Cu systems is that Cu is very reactive and very prone to oxidation, hence can easily form Cu_2O or CuO in the presence of little or excess amount of O_2 in the biofuel and its blend. The recorded variations in the measured TANs for MS and Cu exposed to biodiesel/its blend, corroborate the findings in refs. [10,12]. According to Fazal et al. [13], TAN is indirectly a measure of the degree of the oxidation and also helps to predict the by-products of oxidation, thus an increase in TAN, stirs a corresponding increase in the by-product of oxidation. Also, according to Hoang et al. [7], for fuels, TAN increases due to the presence of corrosive acids which speed-up the corrosion rate of metals in contact with fuels. Kaul et al. [13] recorded differences in TAN values for Al exposed to neat Karanja, Salvadora, Mahua and *Jatropha curcas*, biodiesel fuels; the measured TAN-values of the neat biofuels are 0.42,

0.38, 0.45 and 0.32 (mg KOH/g acid), which gained an alarming increase of 11.30, 2.38, 14.48, 14.39 (mg KOH/g acid), respectively upon contacting the biofuels with Al, thus revealing their relative acidities/tendencies for stimulating corrosion when those biofuels are in contact with Al; these observations are somewhat higher than the results obtained in this study which may be as a result in the difference in the type of oil used, its composition and other inherent properties.

5.2.2. Variation in densities and viscosities

Fig. 7a shows the densities of the fuels before/after contact with the metals at room temperature. For the B100 biofuel, its density (0.820 g/cm^3) remained constant almost all through, thus suggesting that the corrosion products formed after contacting it with Al, Cu and MS did not change. However, for the D100 and B/D-50/50 fuels, there were significant variations in their densities caused by the entrained products of corrosion in the oils; this also justifies the assertion in ref. [18]. Again,

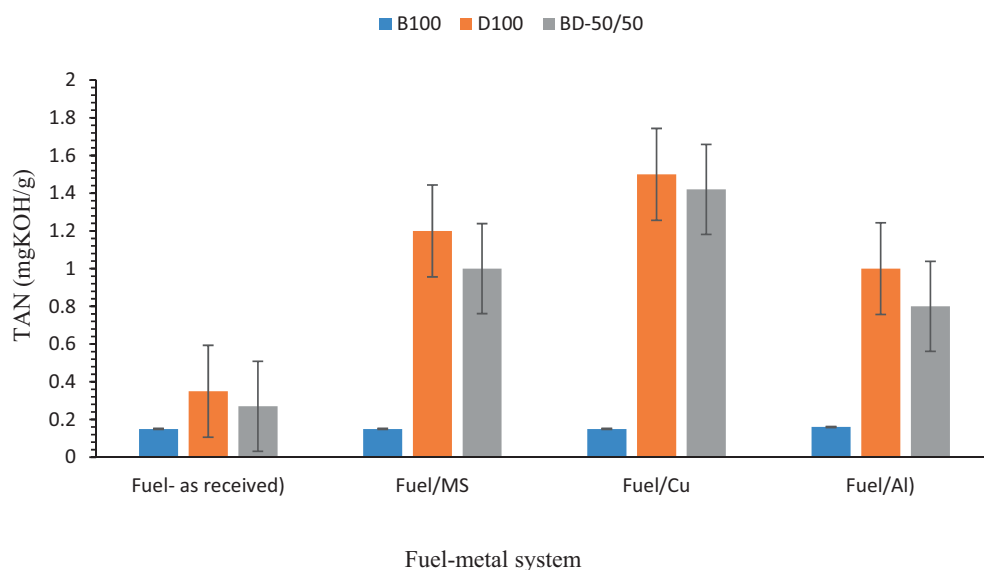


Fig. 6 TAN of fuel blends upon exposure to metal at room temperature.

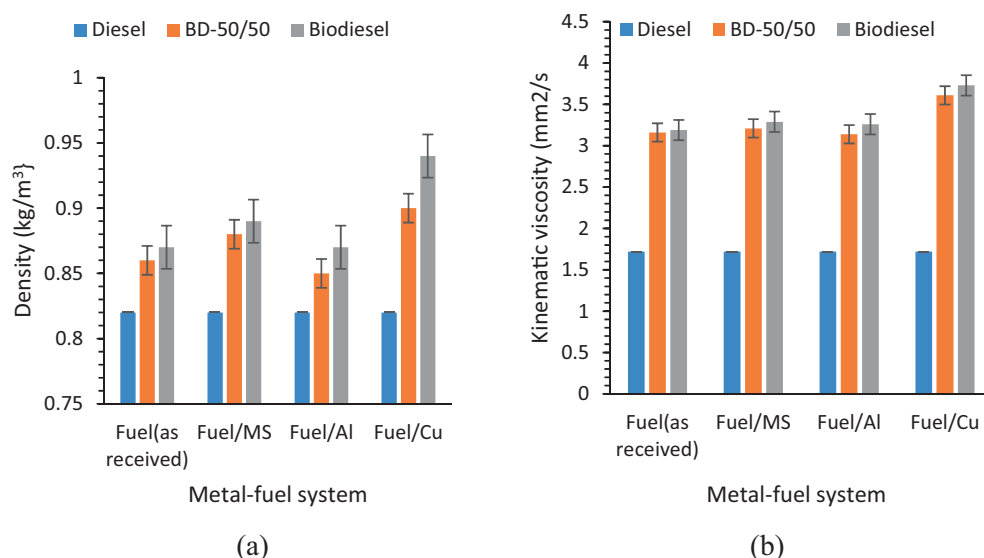


Fig. 7 Variation in fuel properties. (a) Densities (b) Kinematic viscosities within 1200 h of metal-exposure to the fuels at room temperature.

higher densities in the range of 0.9–0.94 g/cm³ were recorded for the Cu -B100, -B/D 50/50 and -D100 fuels, for the MS -B100, -B/D 50/50 and -D100 fuels, the recorded densities range from 0.88 to 0.89 g/cm³, while those of the Cu -B100, B/D 50/50 and D100 fuels, are in the range of 0.85–0.87 g/cm³ as deduced from Fig. 7a. The highest densities recorded for the Cu-fuel system, is due to the very high oxidation tendencies of Cu leading to the entrainment of corrosion products in the fuels, caused by fuel-Cu interactions which had significant influence on the biofuel blend (B/D-50/50) and the biodiesel fuel (D100), as revealed by the ICP device. According to the EN14214 standard, the standard diesel density ranges from 0.86 to 0.9 g/cm³ which is in accordance with the densities recorded for all the fuel-metal systems with the exception of copper due to its higher corrosion tendencies relative to Al

and MS. Since kinematic viscosity equals the ratio of dynamic viscosity to density, it is evident that higher densities inform higher viscosities for the fuel-metal systems shown in Fig. 7b; the higher variation in the viscosities of the D100 and BD-50/50 biofuel-diesel blend are as a result of the higher densities imposed by the corrosion products formed from the metals in contact with the fuels; the order of decreasing viscosities of the fuels is: Cu -B100, -B/D 50/50 and -D100 fuels (1.72, 3.61, 3.73 mm²/s) > MS -B100, -B/D 50/50 and -D100 fuels (1.72, 3.21, 3.29 mm²/s) > Al -B100, -B/D 50/50 and -D100 fuels (1.72, 3.14, 3.26 mm²/s) > the neat fuel systems (B100, B/D-50/50 and D100 - not contacted with the metals) (1.72, 3.16, 3.19 mm²/s). The Cu-fuel systems had the highest viscosities owing to the levels of degradation which caused the density as well as the viscosities of the fuels to increase; this is in accor-

dance with the results in ref. [14]. The viscosities of all the already defined fuel-systems (B100, B/D-50/50 and D100) are greater than the ASTM D6751 viscosity-specification ($2\text{--}6\text{ mm}^2/\text{s}$); this is due to the fact that the micro algae biodiesel and diesel adopted for this study are denser but meet other diesel standard specifications or may require some forms of modification prior use.

The oxidative stabilities of the fuels before and after exposure to Cu, MS and Al are as illustrated in Fig. 8 (a). Since the D100 biodiesel happens to be the most corrosive of the three fuels, this fuel was chosen in order to examine the oxidative stabilities of the three fuels. The induction period (IP) of the D100 biodiesel fuel is 1.22 h, and it reduced to 0.5, 0.64 and 0.89 h after being exposed to the Cu, MS and Al. The results indicate that MS is more resistant to corrosion/oxidation relative to Cu; this also justifies the report on the effect of several inhibitors/bio-oils in reducing the corrosion of MS in diesel/biodiesel as recorded in ref. [15].

The water contents of the fuel/fuel-metal systems are as all illustrated in Fig. 7b. The presence of water in fuel, makes it more aggressive. The B100 and B/D 50/50 fuels have lower water contents relative to that of the pure biodiesel (D100 fuel); like what is expected, the metal in contact with the fuel with the highest water content (i.e., the D100 fuel) should give the highest corrosion rate, however, which is the case for Cu but different for the cases for Al and MS. The reason is because, as seen for the case of Al, despite showing higher water content than MS under the conditions of fuel-metal contact for which the investigations were conducted, the oil-metal interaction forces (i.e., the forces of adhesion of the oil and metal atoms), were more than the forces of adhesion between the metal and water, thus based on the competition between oil and water for the metal-surface, water was repelled from the surface of the metal. Also, the forces of cohesion of the water molecules are higher than the forces of adhesion between the water and Al, thus, the reason for which water penetration or the contribution of water to the corrosion rates of the Al was not evident; also, the formation of an impervious oxide-film could have also savaged Al from the corrosive influence of water. According to literature, 0.05 vol% is the allowable water content for biodiesel fuels [11,19,25–28]. The water contents of all the fuel/fuel-metal systems are: 0.03, 0.037 and 0.04 vol%, 0.1, 0.124 and 0.16 vol%, 0.122, 0.126 and 0.129

as well as 0.17, 0.19 and 0.22 for the neat fuel, Al-fuel, MS-fuel and Cu-fuel systems, respectively. Despite the perceived corrosive influence of water on Cu, the copper-BD-50/50 blend and D100 whose water contents are 0.19 and 0.22 (vol. %) are lower than those recorded in refs. [9,12,17,29–30]. Also, the low water content in MS, is also suggestive of water adsorption in the metal, which may have stimulated higher corrosion rates in MS relative to Al. The elemental compositions of the metals from the XPS analysis before and after corrosion are demonstrated in Table 4.

Based on the results in Table 4, considering the Cu-fuel system, for all the fuels, the metals present in the Cu-metal include C, O, Cu and Pb; there were recorded increases in the carbon (C), oxygen (O) and Pb contents of the Cu -B100, -B/D 50/50 and D100 systems, whereas, the amount of Cu in the Cu-metal decreased after coming in contact with the fuels owing to the high reactivity of copper, hence its conversion to $\text{Cu}_2\text{O}/\text{CuO}$ which is caused by the availability of limited or excess amount of oxygen in the fuels before corrosion relative to what was seen after corrosion. For the Al system, the elements detected include C (which increased), O (which decreased owing to the possible conversion of oxygen to Al_2O_3), and Al, MS which all decreased due to the possibility of some of the nitrogen being adsorbed in the oil thus impeding the corrosive activity of the oil since nitrogen is an inert gas. In addition, there is no doubt that sulphur is corrosive, however, despite its presence in Al, the Al_2O_3 film formed after its contact with fuel, is suspected to be highly resistant to sulphur attack, hence the reason for the insignificant influence of sulphur on Al in the Al-fuel systems. Furthermore, for the MS system, elements such as C, O and Fe were detected and the amount of C increased, while those of oxygen and Fe decreased and this is as a result of the high tendency of Fe to react with oxygen to form a corrosion product (Fe_2O_3) which is reddish brown in nature; the compound is also a product of oxidation of MS.

5.3. Characterization of corrosion products.

5.3.1. Morphology of corrosion products

Fig. 9 illustrates the SEM micrographs of the different fuel/fuel-metal systems not exposed/exposed to MS, Al and Cu surfaces at 60 °C. Surface damages exist as a result of corrosion

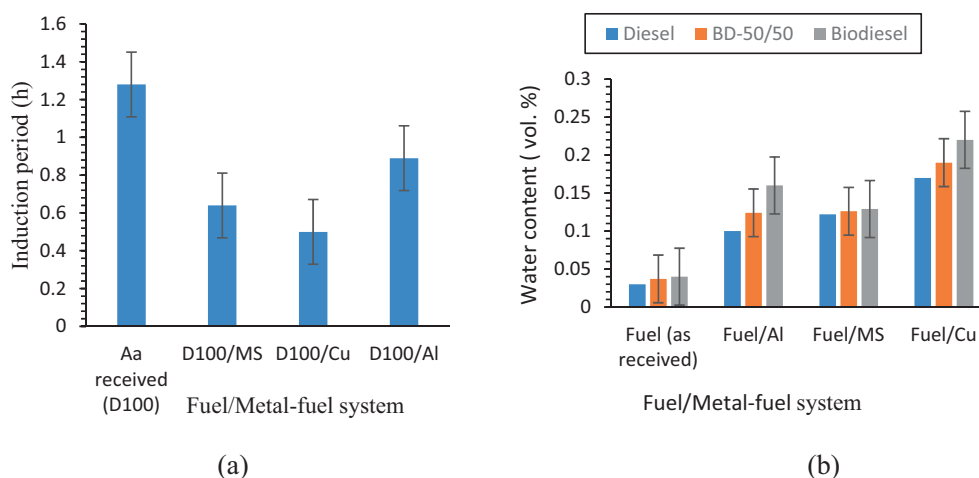


Fig. 8 (a) Oxidation stability; (b) Water content of fuels within 1200 h of exposure to metal at room temperature.

Table 4 Elemental composition of metal surface in contact with diesel, biodiesel and BD50-50(blends) before and after corrosion.

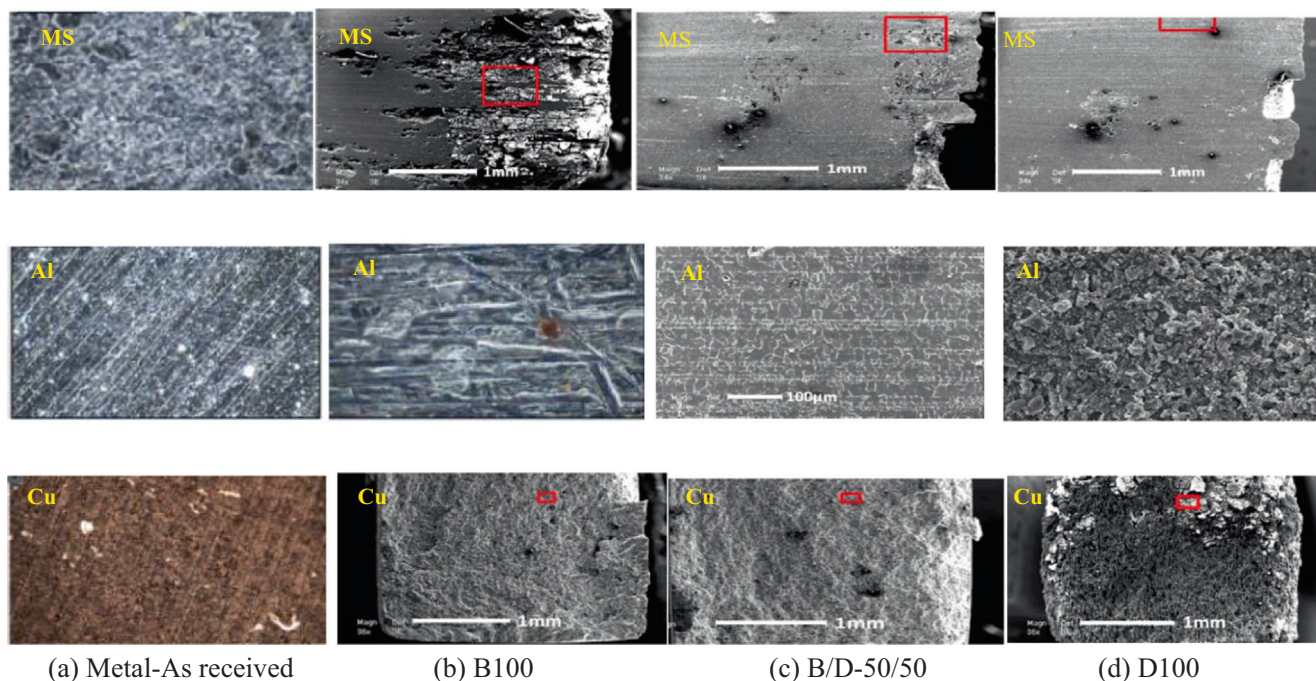
Parameter	Diesel					Biodiesel					Blend				
	C	O	Cu	Pb		C	O	Cu	Pb		C	O	Cu	Pb	
Cu % (at% ^a)															
BC	40.2	26.7	33.1	0		40.2	26.7	33.1	0		40.2	26.7	33.1	0	
AC	49.8	32.7	17.3	0.2		56.1	39.2	4.18	0.52		53.7	35.3	10.62	0.38	
Al % (at% ^a)															
BC	33.3	51.0	8.1	6.5	1.1	33.3	51.0	8.1	6.5	1.1	33.3	51.0	8.1	6.5	1.1
AC	45.7	47.9	7.1	0.1	0.1	44.1	50.2	6.7	0	0	45.2	48.0	6.8	0	0
MS (at% ^a)															
BC	25.7	51.4	22.9			25.7	51.4	22.9			25.7	51.4	22.9		
AC	38.3	45.7	16			42.5	44.1	13.4			40.7	44.9	14.4		

BC = Before corrosion; AC = After corrosion.

^a at% – atomic percentage of metal element.

on the metal surfaces exposed to biodiesel, diesel, and the blend as compared to the surface of metals which had no contact with the fuels. After the immersion tests, the more visible pits marked by red boxes on the metal surfaces exposed to biodiesel or its blends are due to the higher induced rates of corrosion imposed by the fuels on the metals. The surface of Cu in contact with biodiesel shows the highest presence of pits compared to those of MS and Al; the existence of a black coloration on the surface of Cu after contact with the fuels is indicative of the formation of Cu_2O which is black in color. Fazal et al. [13], reported that Cu in oxygen produces an oxygen-rich Cu_2O (inner layer) and an outer CuO/CuCO_3 (outer layer). They also asserted that when biodiesel is exposed

to the surface of Cu, pits are formed as a result of the replacement of O_2 ions from Cu_2O during the destruction of the CuO -layer on the Cu-surface. The higher percentage of Cu (black color) and O_2 on the Cu-surface are as a result of the nature/elemental composition of the oxide layer. Oxygen concentration for the Cu-metal system increased with static test immersion-time, whereas, the reverse was the case for the Al and MS-fuel systems. Norouzi et al. [31], suggested that the oxide layer formed on the Cu-metal surface when in contact with fuels, is as a result of the metal's exposure to oxygen. The carbon content of the Al -B100, -B/D 50/50 and MS -B100, -B/D 50/50 systems increased, owing to the significant reduction in the composition of the other elements i.e., O


Fig. 9 Morphology of: (a) copper, (b) mild steel and (c) aluminum after exposure to biodiesel, diesel, biodiesel-diesel blends at 60 °C. *Each column section from the left, represents the SEM image for the neat metal, B100-, B/D-50/50- and D100- metal systems.

and Fe. This is because, by proportion, since carbon by nature, is unsusceptible to corrosion, its value by proportion increased because, its composition remained constant while other elements reduced. Fazal et al. [7,13] reported that biodiesel oxidation can lead to different fatty acid formation, which can increase its corrosivity/the tendency to form several metal oxides. This is also evident in the few marked red boxes on the as-received images of the neat metals, although more predominant in the metal contacted with D100, compared to those contacted with B100 and BD-50/50 fuels. The rough surfaces of the Al- and MS (B100 and -B/D 50/50) -contacted metals, are also not as predominant as those evident in the Cu (B100, B/D 50/50) systems. However, the pit densities in Al is less than those of MS and Cu for all the metal-fuel systems.

The EDX spectra in Fig. 10 justifies the elemental distribution of the systems presented in Table 4 for the worst fuel-metal system (D100). Fig. 9, AFM images measures the mechanical properties of a sample of biodiesel exposed to (a) Cu, (b) MS and (c) Al surfaces after 1200 h of exposure to metals at 60 °C. The elemental distribution of the metals in the metal samples were examined at a wavelength range of $R_a = 244.492$ nm for the Cu-D100 metal-fuel system, 208.116 nm for the MS- D100 metal-fuel system and 188.875 nm for Al- D100 metal-fuel system, respectively. These results are complementary to those observed for the SEM micrographs in Fig. 9.

The metals in contact with fuels show more corrosion attacks as seen in their surface roughness from Atomic force

Microscopy (AFM) (Fig. 11). The order of roughness of the metals is in the following decreasing order: $Cu > MS > Al$.

The composition/compositional changes in Table 5, show the *Schinzochytrium* sp. biodiesel methyl esters before and after contact with Cu/MS/Al for 1200 h. Palmitoleic acid, Stearic acid, and linolenic acid are the major free fatty acids (FFAs) in the *Schinzochytrium* sp., which reduced in concentration after prolonged exposure to Cu, Al and MS for 1200 h. Some components, such as Gadoleic acid and Docosatrienoic acid, were also produced; meanwhile, Behenic acid and Erucic acid, increased in terms of concentration. Hence, there is need to focus future research on understanding the mechanisms responsible for the change in composition of biodiesel, formation of the aforementioned acids as well as their effect on the fuel's properties.

The SAED patterns of some specific regions in Al, MS and Cu are shown in Fig. 12. The SAED patterns, show the presence of MS, Al and Cu peaks in the spectra. The SAED indicates the crystalline nature of the metal surface.

The different diffraction patterns exhibited by the D100-metal systems are as indicated in Fig. 12 a-c. Very sharp/obvious diffractions or response to photon energy are seen to be very prominent on the surface of the Cu-D100 metal-fuel system as a result of the existence of mobile ions on the surfaces of the Cu induced by corrosion. The order of diffraction of light as it travels in air through the dense corrosion layers is: $Cu > MS > Al$, which also justifies the order of the recorded

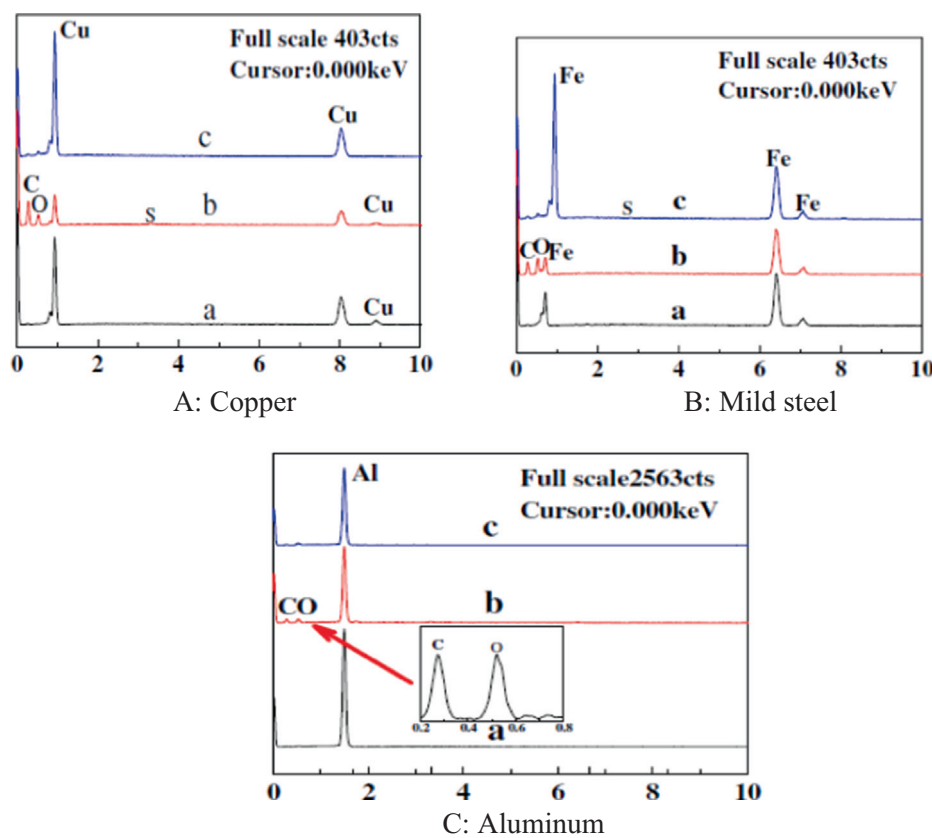


Fig. 10 EDX spectra of the metals after corrosion at 60 °C: (A) Cu, (B) MS, (C) Al.

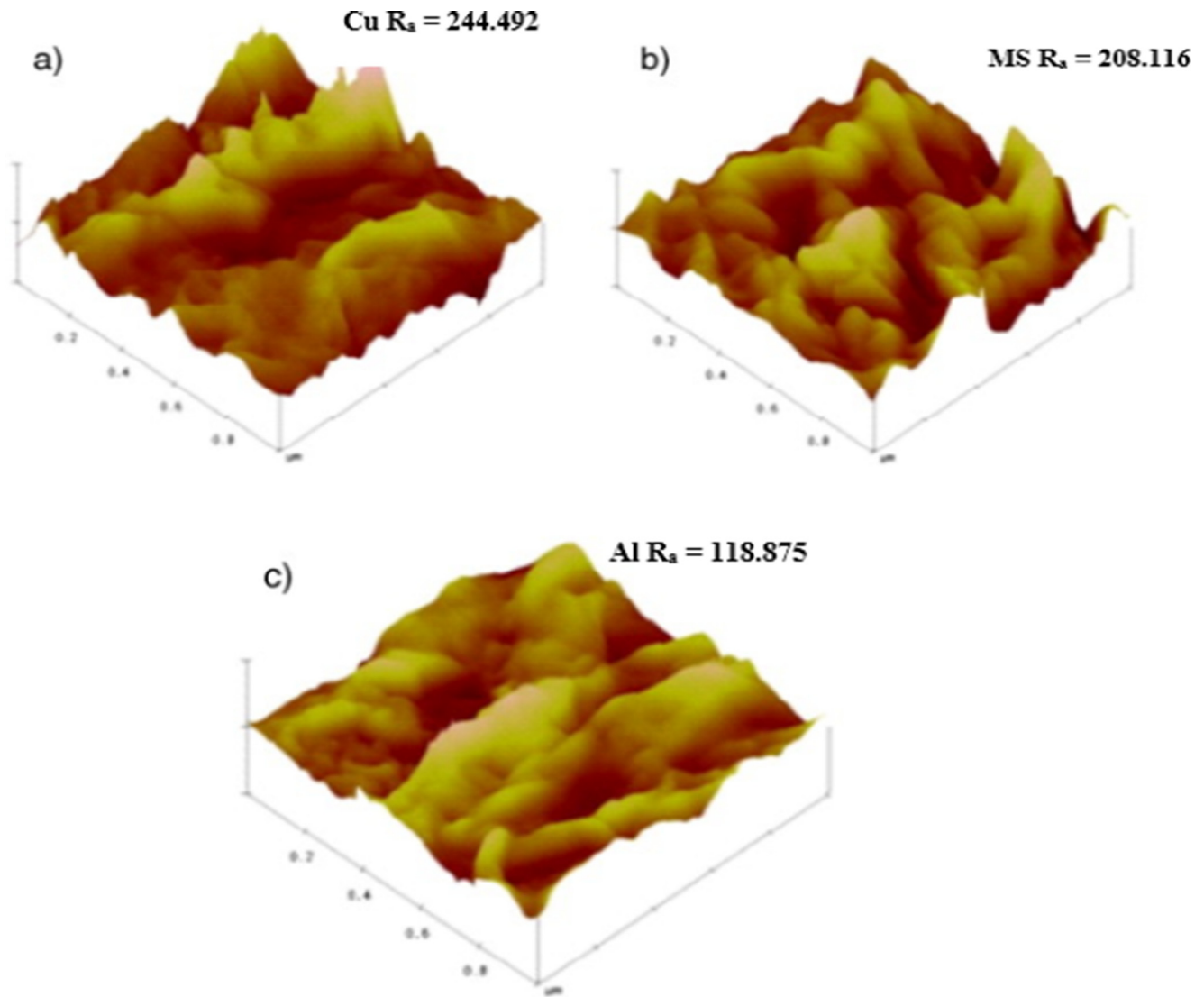


Fig. 11 Surface roughness of the: (a) Cu in contact with Cu-D100 system, (b) MS in contact with MS-D100 system, (c) Al in contact with Al-D100 system.

corrosion rates for the metals when in contact with the D100 fuel as seen in Fig. 6b and c.

Fig. 13, shows the sintered TEM (Transmission Electron Microscopy) analysis of A (as received), B (D100/MS); C (D100/Cu) and D (D100/Al). The TEM images confirm the presence of MS, Al and Cu. This coincides with the results of the already reported SEM and AFM spectra for these metals. The presence of dislocations is indicated by the black arrows on the metal surfaces. This dislocation occurs as a result of the mismatch that exists between the Al/MS/Cu matrices imposed by the fuels.

Another reliable technique for corrosion monitoring of metals when exposed to biodiesel is XRD analysis as illustrated in Fig. 14. Before immersion in the biodiesel, Cu, Fe and Al were detected in the neat metals, however after contacting the metals with the fuels, the products of metal-degradation, such as Fe_2O_3 , CuO , FeO(OH) , Cu(OH)_2 , AlO(OH) , and FeCO_3 were rarely noticed. Nevertheless, after immersion in biodiesel, higher concentrations of copper were

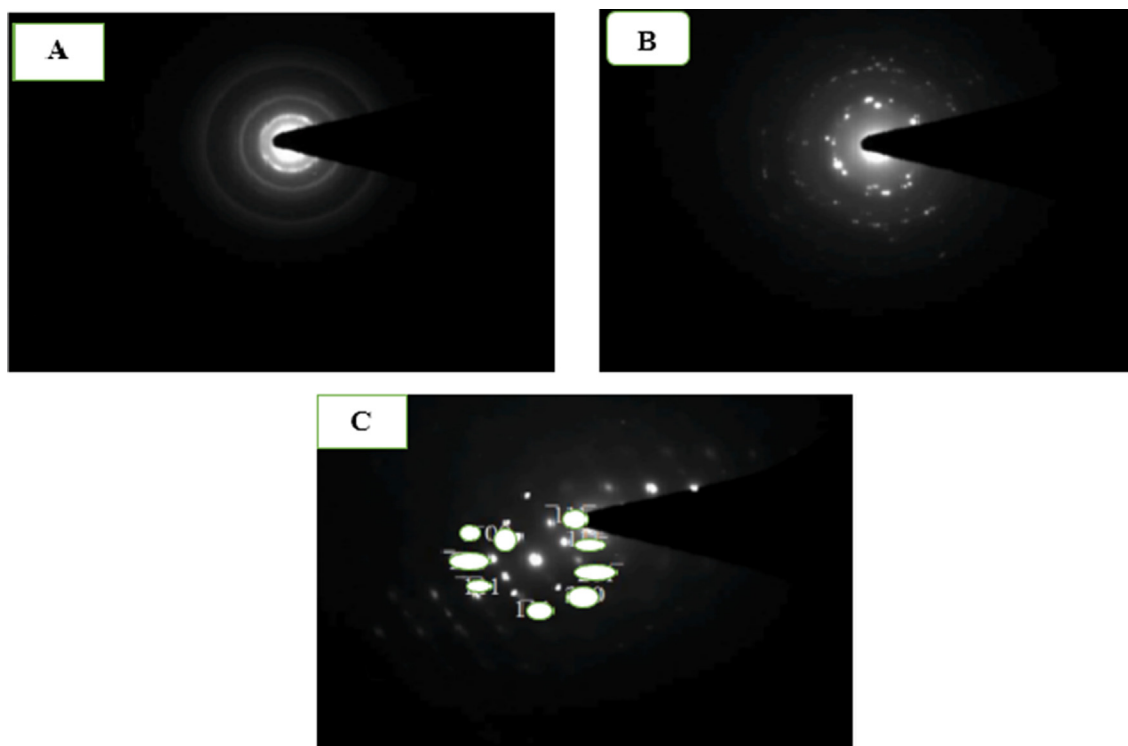
observed, which are suggestive of the occurrence of Cu(OH)_2 and CuCO_3 , CuO , and FeO that may have ensued from copper/MS corrosion as observed in ref. [9]. An increase in temperature from room temperature to 60°C , may have resulted in the high frequency of peaks that were suggestive/indicative of the corrosion products (Fe_2O_3 , CuCO_3 , Cu(OH) , FeO(OH) , CuO , FeCO_3 and AlO(OH)), which are seen in the XRD-patterns caused by the influence of temperature; this is in line with the findings in refs. [4,13,16].

5.4. Statistical analysis

Fig. 15 illustrates the statistical data of for corrosion rate against reaction time using the Minitab software which helps to predict the effect of corrosion rates of preheated *Schizochytrium* sp. microalgae biodiesel on metallic components of a diesel engine. The standard deviation and coefficient of variance for the reaction time are 345.2 and 47.95, and that of corrosion rate are 0.0801 and 62.37 respectively, Table 6

Table 5 FFA composition from GCMS, for *Schinzoxytrium* sp. biodiesel before and after exposure to the metals.

Fatty acid	Formula	D100	D100/Al	D100/Cu	D100/MS
Myristic acid	C14:0	0.2	0.1	0.2	0.1
Palmitic acid	C16:0	0.1	0.2	–	0.3
Palmitoleic acid	C16:1	35.82	34.97	29.99	33.73
Stearic acid	C18:1	13.01	11.01	10.93	11.58
Oleic acid	C18:1	2.2	2.5	2.6	2.4
Linolenic acid	C18:3	24.27	23.28	22.52	23.09
Gadoleic acid	C20:1	0.3	0.7	0.6	0.8
Eicosatrienoic acid	C20:3	–	0.1	0.2	–
Arachidonic acid	C20:4	0.3	–	–	–
Behenic acid	C22:0	0.1	0.1	0.3	0.2
Clupanodonic acid	C22:2	–	0.1	0.1	–
Docosatrienoic acid	C22:3	1.9	3.7	4.9	3.1
Lignoceric	C24:0	0.2	–	–	0.1
Nervonic acid	C24:1	1.6	2.9	–	–
Erucic acid	C22:1	0.1	0.3	–	0.2
Squalene	C30:1	–	0.1	0.3	–

**Fig. 12** Selected diffraction patterns of (a) D100/MS (b) D100/Al, (C) D100/Cu.

shows other statistical parameter such as the skewness, sum of square, etc.

6. Conclusion

Presently, biodiesel in its pure state is not used for commercial purposes as a result of concerns which lead to the failure of

metallic components of diesel engines which subsequently result in metal-degradation. Biodiesel can induce high levels of corrosion of the engine-parts of diesel engines, caused by fuel-metal contact. Thus, preventing the negative effects and understanding the mechanisms resulting in the corrosion of machine parts in the engines, is a big task for manufacturers, scientists, and engineers. The corrosion characteristics of diesel engine-parts made of Cu, Al and MS were examined both at

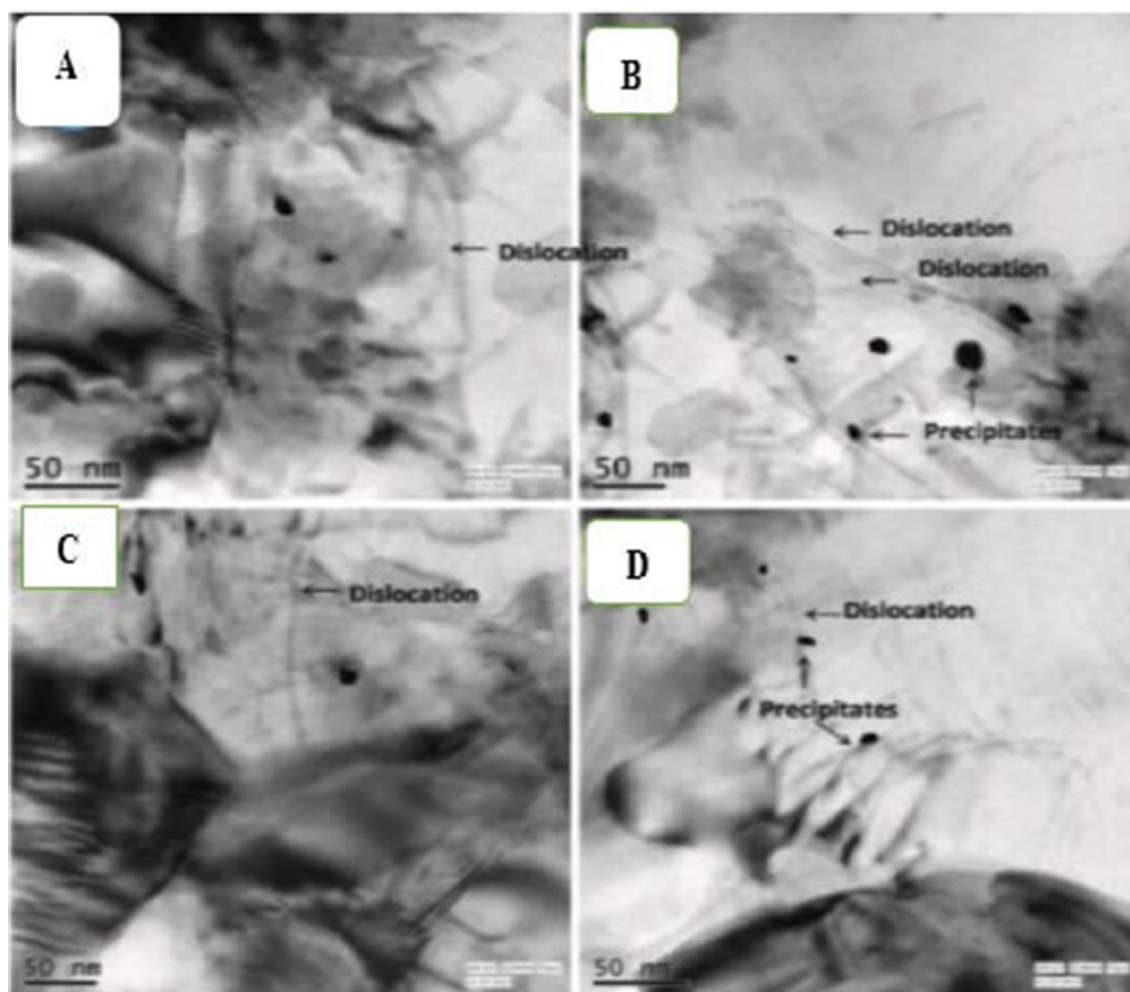


Fig. 13 TEM images of the selected area electron diffraction (SAED) patterns for (a) Al, (b) MS (c) MS and (d) Neat MS as control.

room temperature (27 °C) and at 60 °C for 1200 h via static immersion tests. Fuel and metal degradation were somewhat evident in all cases of fuel-metal contacts. Hence, the major conclusions from the current investigation are as follows:

- (a) Unblended/pure biodiesel is the most corrosive fuel amongst all the three fuels contacted with Cu, MS and Al.
- (b) Cu is highly susceptible to oxidation in *Schinzochytrium* sp. microalgae biodiesel, its blend and the conventional diesel fuel.
- (c) The presence of O₂ moieties, high moisture, and fatty acids increased the corrosion tendencies of the metals when contacted with the B100 and B/D-50/50 fuels.
- (d) When the biodiesel or its blends come in contact with Al, MS and Cu, there is significant degradation in the properties of the fuels as indicated by increasing densities, TAN-rates, and viscosities of the fuels.
- (e) Despite having some measure of compatibility with biodiesel, mild steel is susceptible to changes in properties of the fuel as well.
- (f) Of all the metals, Al is the most resistant to diesel, bio-fuel or diesel-biofuel fractions whereas, the least resistant metal to fuel-induced corrosion is Cu.
- (g) At room temperature/60 °C Cu has the highest corrosion rate in neat biodiesel (D –100) at 0.37 and 0.69 mpy respectively. However, at the same temperatures condition, the lowest corrosion rate occurs in (B –100) for Al at 0.07 and 0.14 mpy.

Declaration of Competing Interest

The authors declare that they have no known competing financial interests or personal relationships that could have appeared to influence the work reported in this paper.

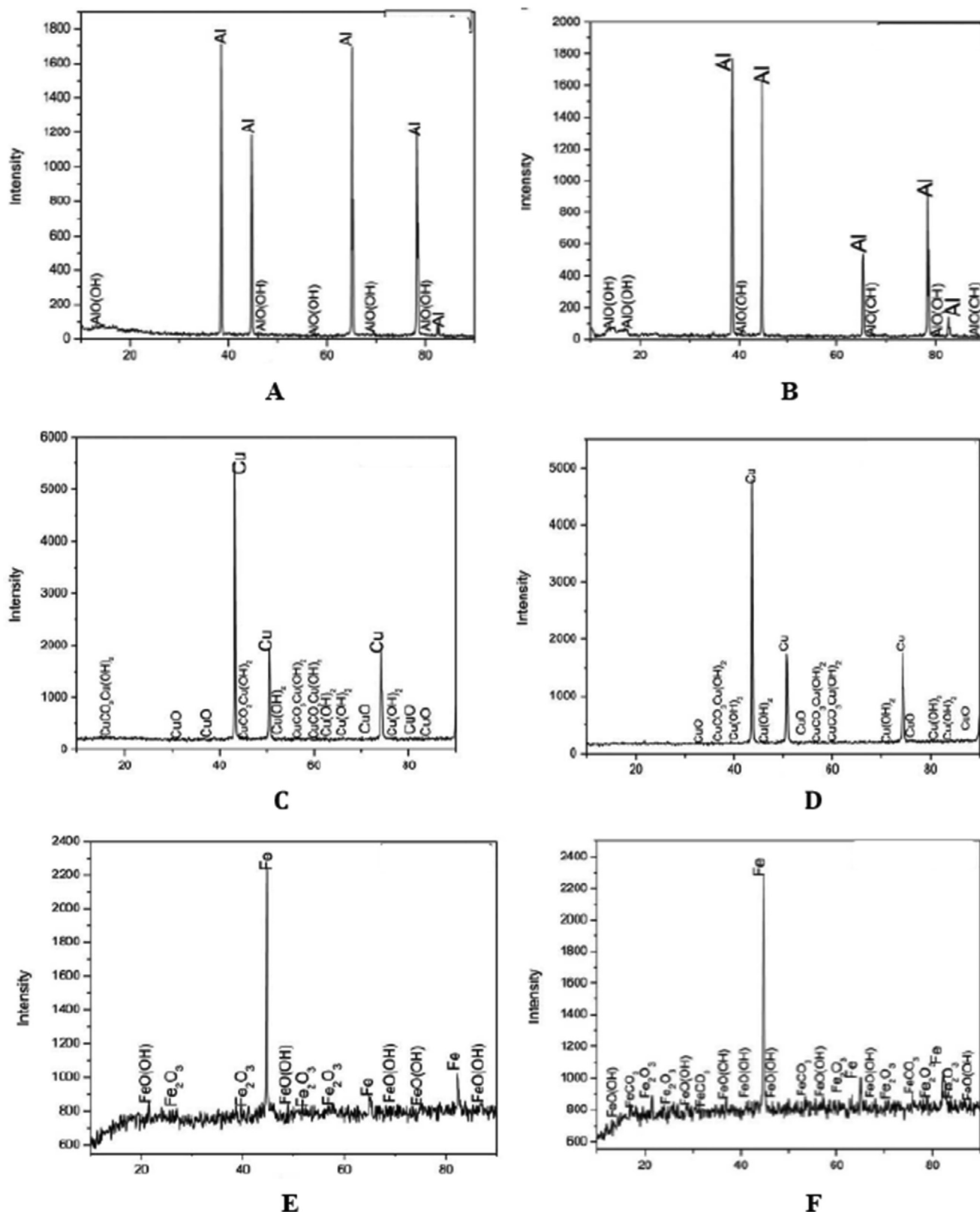


Fig. 14 XRD Patterns of: (A) before immersion of Al (B) After immersion of Al; (C) before immersion of Cu (D) After immersion of Cu (E) before immersion of MS (F) After immersion of MS in the D100 fuel system.

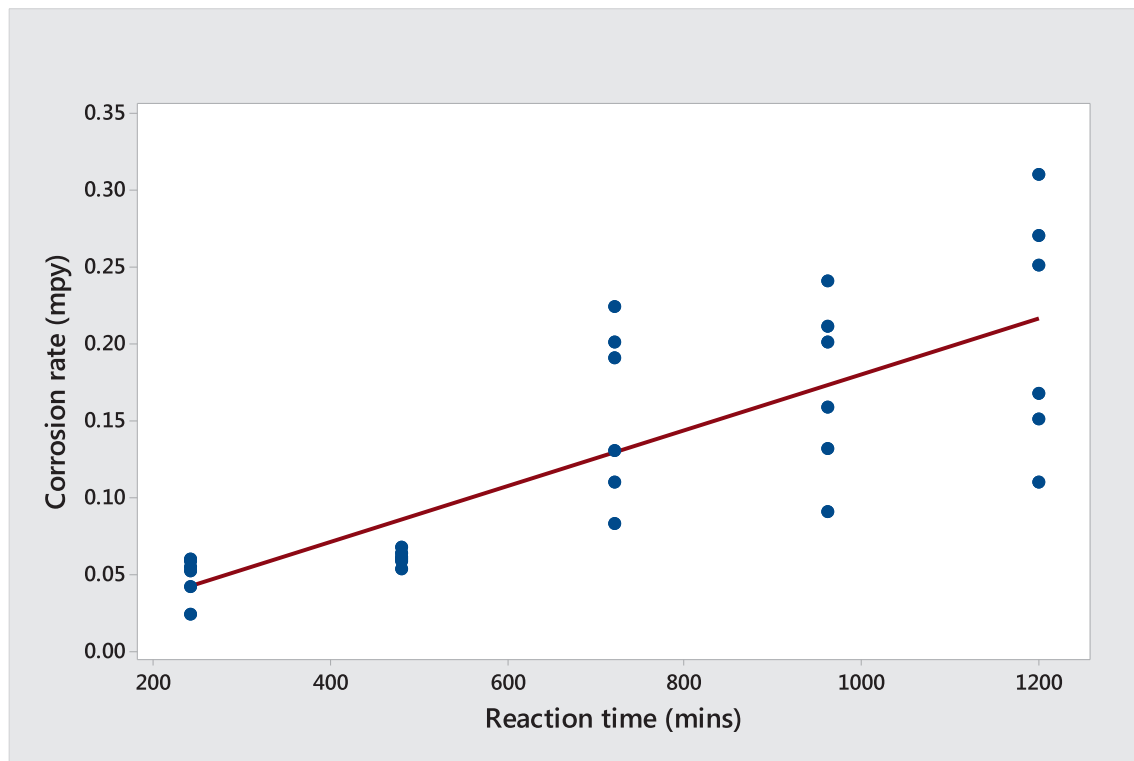


Fig. 15 Linear plot of corrosion rate (mpy) versus reaction time (min).

Table 6 Statistical data generated for corrosion rates of preheated *Schinzochytrium* sp. microalgae biodiesel on metallic components of a diesel engine.

Variable	N	Mean	SE Mean	St.Dev	Variance	Coef. Var	Sum	Sum of Squares	Q1	Median	Q3	Max.	Skewness
Reaction time (mins)	30	720.0	63.0	345.2	119172.4	47.95	21600.0	19008000.0	480.0	720.0	960.0	1200.0	-0.00
Corrosion rate (mpy)	30	0.1285	0.0146	0.0801	0.0064	62.37	3.8550	0.6817	0.0578	0.1090	0.2000	0.3100	0.63

Acknowledgement

Authors wish to appreciate Covenant University, Ota, Nigeria and OBA1 auto services group limited, Nigeria for their support at the experimental stage and an anonymous organization for helping in carrying out all sample-characterization/analysis.

References

- [1] M. Elkelawy, H.A. Bastawissia, K.K. Esmail, A.M. Radwan, H. Panchal, K.K. Sadasivuni, M. Suresh, M. Israr, Maximization of biodiesel production from sunflower and soybean oils and prediction of diesel engine performance and emission characteristics through response surface methodology, *Fuel* 266 (2020) 117072.
- [2] X.P. Nguyen, H.N Vu, Corrosion of the metal parts of diesel engines in biodiesel- based fuels; *Int. J. Renew. Energy Develop.* 8(2) (2019) 119–132.
- [3] A. Singh, S. Sinha, A.K. Choudhary, H. Panchal, M. Elkelawy, K.K. Sadasivuni, Optimization of performance and emission characteristics of CI engine fueled with *Jatropha* biodiesel produced using a heterogeneous catalyst (CaO), *Fuel* 280 (2020) 118611.
- [4] A.T. Hoang, V.D. Tran, V.H. Dong, A.T. Le, An experimental analysis on physical properties and spray characteristics of an ultrasound-assisted emulsion of ultra-low-sulphur diesel and *Jatropha*-based biodiesel, *J. Marine Eng. Technol.* (2019), <https://doi.org/10.1080/20464177.2019.1595355>.
- [5] S.C. Sekhar, K. Karuppasamy, N. Vedaraman, A.E. Kabeel, R. Sathyamurthy, M. Elkelawy, Biodiesel production process optimization from *Pithecellobium dulce* seed oil: Performance, combustion, and emission analysis on compression ignition engine fueled with diesel/biodiesel blends, *Energy Convers. Manage.* 161 (2018) 141–154.

- [6] A.T. Hoang, A.T. Le, V.V. Pham, A core correlation of spray characteristics, deposit formation, and combustion of a high-speed diesel engine fueled with Jatropha oil and diesel fuel. *Fuel* 244 (2019) 159–175.
- [7] Anh Tuan Hoang, Van Viet Pham, A study of emission characteristic, deposits, and lubrication oil degradation of a diesel engine running on preheated vegetable oil and diesel oil. *Energy Sourc., Part A: Rec. Utilizat. Environ. Effect.* (2018) 1–15. <https://doi.org/10.1080/15567036.2018.1520344>.
- [8] M.A. Fazal, A.S.M.A. Haseeb, H.H. Masjuki, A critical review on the tribological compatibility of automotive materials in palm biodiesel. *Energy Convers. Manage* 79 (2014) 180–186.
- [9] S.K. Singh, A.K. Agarwal, M. Sharma, Experimental investigations of heavy metal addition in lubricating oil and soot deposition in an EGR operated engine, *Appl. Therm. Eng.* 26 (2–3) (2006) 259–266, <https://doi.org/10.1016/j.applthermaleng.2005.05.004>.
- [10] A.K. Agarwal, A. Dhar, Karanja oil utilization in a direct-injection engine by Preheating. Part 2: Experimental investigations of engine durability and lubricating oil properties, *Proc. Inst. Mech. Eng. Part D: J. Automob. Eng.* 224(1) (2010) 85–97. London, UK: Sage Publications.
- [11] D. Agarwal, S.K. Singh, A.K. Agarwal, Effect of exhaust gas recirculation (EGR) on performance Emissions, Deposits and Durability of a Constant Speed Compression Ignition Engine, *Appl. Energy* 88 (8) (2011) 2900–2907, <https://doi.org/10.1016/j.apenergy.2011.01.066>.
- [12] A.T. Hoang, Experimental study on spray and emission characteristics of a diesel engine fueled with preheated biooils and diesel fuel, *Energy* 171 (2019) 795–808.
- [13] M.A. Fazal, M.R. Jakeria, A.S.M.A. Haseeb, Effect of copper and mild steel on the stability of palm biodiesel properties: a comparative study, *Ind. Crop. Prod.* 58 (2014) 8–14.
- [14] M.A. Fazal, A.S.M.A. Haseeb, H.H. Masjuki, Degradation of automotive materials in palm biodiesel, *Energy* 40 (2012) 76–83.
- [15] A.L. Squizzato., T.S. Neri., N.M.M. Coelho, E.M. Richter, R. A.A. Munoz, In situ electrochemical determination of free Cu (II) ions in biodiesel using screen-printed electrodes: direct correlation with oxidation stability. *Fuel* 234 (2018) 1452–1458. <https://doi.org/10.1016/j.fuel.2018.08.027>.
- [16] A.S.M.A. Haseeb, M.A. Fazal, M.I. Jahirul, H.H. Masjuki, Compatibility of automotive materials in biodiesel: a review, *Fuel* 90 (2011) 922–931.
- [17] S. Kaul, R.C. Saxena, A. Kumar, M.S. Negi, A.K. Bhatnagar, H.B. Goyal, A.K. Gupta, Corrosion behaviour of biodiesel from seed oils of Indian origin on diesel engine parts, *Fuel Process. Technol.* 88 (2007) 303–307.
- [18] M.A. Fazal, A.S.M.A. Haseeb, H.H. Masjuki, Comparative corrosive characteristics of petroleum diesel and palm biodiesel for automotive materials, *Fuel Process. Technol.* 91 (2010) 1308–1315.
- [19] A.S.M.A. Haseeb, H.H. Masjuki, L.J. Ann, M.A. Fazal, Corrosion characteristics of copper and leaded bronze in palm biodiesel, *Fuel Process. Technol.* 91 (2010) 329–334.
- [20] M.A. Fazal, A.S.M.A. Haseeb, H.H. Masjuki, Corrosion mechanism of copper in palm biodiesel, *Corro. Sci.* 67 (2013) 50–59.
- [21] S.A. Md, M.B.H. Hassan, M.d. Abul Kalam, Comparative corrosion characteristics of automotive materials in Jatropha biodiesel, *Int. J. Green Energy* (2018), <https://doi.org/10.1080/15435075.2018.1464925>.
- [22] E. Hu, Y. Xu, X. Hu, L. Pan, S. Jiang, Corrosion behaviors of metals in biodiesel from rapeseed oil and methanol, *Renew. Energ.* 37 (2012) 371–378.
- [23] D.L. Cursaru, G. Branoiu, I. Ramada, F. Miculescu, Degradation of automotive materials upon exposure to sunflower biodiesel, *Ind. Crop. Prod.* 54 (2014) 149–158.
- [24] B.A. Oni, S.E. Sanni, Michael Daramola, A.V. Olawepo, Effects of oxy-acetylation on performance, combustion and emission characteristics of *Botryococcus braunii* microalgae biodiesel-fuelled CI engines, *Fuel* 296 (2021) 120675.
- [25] A.L. Squizzato., T.S. Neri, N.M.M. Coelho, E.M. Richter, R.A. A. Munoz, In situ electrochemical determination of free Cu(II) ions in biodiesel using screen-printed electrodes: direct correlation with oxidation stability. *Fuel* 234 (2018) 1452–1458. <https://doi.org/10.1016/j.fuel.2018.08.027>.
- [26] M.A. Fazal, A.S.M.A. Haseeb, H.H. Masjuki, Effect of temperature on the corrosion behavior of mild steel upon exposure to palm biodiesel, *Energy* 36 (2011) 3328–3334.
- [27] K.V. Chew, A.S.M.A. Haseeb, H.H. Masjuki, M.A. Fazal, M. Gupta, Corrosion of magnesium and aluminum in palm biodiesel: a comparative evaluation, *Energy* 57 (2013) 478–483.
- [28] R. Sanchez, C. Sanchez, C.P. Lienemann, J.L. Todoli, Metal and metalloids determination in biodiesel and bioethanol, *J. Anal. At. Spectrom.* 30 (2015) 64–101.
- [29] A.T. Hoang., A.T. Le, V.V. Pham, Impact of jatropha oil on engine performance, emission characteristics, deposit formation, and lubricating oil degradation, *Combust. Sci. Technol.* 191(2) (2018) 1–16.
- [30] A.T. Hoang, M.T.M. Aghbashlo, A review of the effect of biodiesel on the corrosion behaviour of metals/alloys in diesel engines, *Energy Sourc. Part A: Recov. Utilizat. Environ. Effect.* (2019). <https://doi.org/10.1080/15567036.2019.1623346>.
- [31] S. Norouzi, F. Eslami, M.L. Wysynski, A. Tsolakis, Corrosion effects of RME in blends with ULSD on aluminum and copper, *Fuel Process. Technol.* 104 (2012) 204–210.